available at www.sciencedirect.com

ScienceDirect

journal homepage: www.elsevier.com/locate/compag

Mapping sunflower yield as affected by *Ridolfia segetum* patches and elevation by applying evolutionary product unit neural networks to remote sensed data

P.A. Gutiérrez[b], *F. López-Granados*[b], *J.M. Peña-Barragán*[b,*], *M. Jurado-Expósito*[b], *M.T. Gómez-Casero*[b], *C. Hervás-Martínez*[a]

[a] *Department of Computing and Numerical Analysis, University of Cordoba, Campus de Rabanales, 14071 Cordoba, Spain*
[b] *Institute for Sustainable Agriculture, C.S.I.C., 14080 Cordoba, Spain*

ARTICLE INFO

Article history:
Received 7 February 2007
Received in revised form
18 July 2007
Accepted 20 July 2007

Keywords:
Remote sensing
Artificial neural networks
Yield prediction
Evolutionary algorithms
Sunflower

ABSTRACT

Recent advances in remote sensing technology have triggered the need for highly flexible modelling methods to estimate several crop parameters in precision farming. The aim of this work was to determine the potential of evolutionary product unit neural networks (EPUNNs) for mapping in-season yield and forecasting systems of sunflower crop in a natural weed-infested farm. Aerial photographs were taken at the late vegetative (mid-May) growth stage. Yield, elevation and weed data were combined with multispectral imagery to obtain the dataset. Statistical and EPUNNs approaches were used to develop different yield prediction models. The results obtained using different EPUNN models show that the functional model and the hybrid algorithms proposed provide very accurate prediction compared to other statistical methodologies used to solve that regression problem.

1. Introduction

One aspect of overcoming the possibility of minimizing the impact of agriculture on environmental quality is the development of more efficient approaches for crop production. The site-specific application of agricultural inputs (e.g., fertilizer or herbicide) based on accurate field maps is an essential component of the successful implementation of precision farming, leading to a reduction in the overall quantities applied (Karimi et al., 2005). Although the benefits obtained through yield mapping depend largely on the crop and the environmental conditions (Yang et al., 2000a), harvester-mounted crop yield monitoring systems are now being extensively used by farmers to maximize the yields under highly variable field conditions (Uno et al., 2005). As a first step to finding out the field variability, yield maps play an important role in the decision making process in precision agriculture.

One of the main field characteristics causing yield variability is the field topography or elevation (Kravchenko and Bullock, 2002a,b). Several authors have reported that the Elevation affects the spatial variability of yield (Kravchenko and Bullock, 2002a; Pilesjö et al., 2005) and weed intensity (Jurado-Expósito et al., 2005; Liu et al., 2002).

Sunflower (*Helianthus annuus* L.) is one of the most abundant crops in Andalusia, Southern Spain, grown on over 320,000 ha annually. It is usually grown under dry land conditions; sowing time is February–March and harvesting time July–August. *Ridolfia segetum* Moris is an umbelliferous weed, which is frequent and abundant in clay soils in Andalusia. Once established, the growth rate of *R. segetum* is very

* Corresponding author. Tel.: +34 957 499 219; fax: +34 957 499 252.
E-mail address: pa2pebaj@uco.es (J.M. Peña-Barragán).
0168-1699/$ – see front matter © 2007 Elsevier B.V. All rights reserved.
doi:10.1016/j.compag.2007.07.011

rapid and its life cycle coincides with that of sunflower yield, which enhances the competitive ability of weed and results in an average yield reduction of about 32% when infestation is two *R. segetum* plants m^{-2} (Castro-Tendero and García-Torres, 1995; Carranza et al., 1995; Peña-Barragán et al., 2006). Although weed control is commonly achieved with pre-planting incorporated and pre-emergence herbicides, none of these herbicides control *R. segetum* and consequently post-emergence tillage or hand-weeding are frequently used to control this weed. Classical competition models not taking into account the spatial component of *R. segetum* infestations were developed by Carranza et al. (1995).

Remote sensing systems can provide a large amount of continuous field information at a reasonable cost, offering great advantages to understand the yield maps created by the harvester-mounted yield-monitoring units (Uno et al., 2005). The importance of remote sensing in site-specific agriculture has been widely reviewed for yield mapping of different crops (Plant, 2001; Yang et al., 2001, 2006). Remotely sensed imagery shows great potential in establishing the impact of seasonally changeable factors (e.g., precipitation, temperature and sunshine) in crop production (Uno et al., 2005), therefore one of the main challenges of remote imagery analysis is to determine how variations in the spectral information are related to differences in the crop state, in order to predict accurate yield maps long before the harvest. Peña-Barragán et al. (2007) obtained maps of *R. segetum* patches in sunflower using aerial photography, taking into account specific timeframes. However, no information has been found about the yield estimation of sunflower considering the presence of *R. segetum* patches and their multispectral characteristics on a field scale.

Different statistical, artificial intelligence and machine learning algorithms have proved to be quite useful in the interpretation of remotely sensed data. Kenkel et al. (2002) reported that multivariate statistical approaches have only recently started to be used in agricultural domain. The application of discriminant analysis to agricultural remote sensing in weed discrimination has been reported in many recent studies (Burks et al., 2002; Cho et al., 2002). Furthermore, the stepwise multiple linear regression (SMLR) is one of the most commonly used multivariate analytical techniques to develop empirical models from large data sets, as has been done for a number of canopy-level crop condition parameters (Shibayama and Akiyama, 1991; Osborne et al., 2002). This model fitting process is quite stable, resulting in low variance but in a potentially high bias. A traditional technique to overcome these difficulties is augmenting/replacing the input vector with new variables, the basis functions, which are transformations of the input variables and then using linear models in this new space of derived input features. Methods like artificial neural networks (ANNs) (Bishop, 1995), projection pursuit learning (Friedman and Stuetzle, 1981) and generalized additive models (Hastie and Tibshirani, 1990), can be seen as different basis function models.

Approaches based on ANNs have been applied in agricultural remote sensing (Goel et al., 2003; Karimi et al., 2005; Shanin et al., 2002; Uno et al., 2005; Yang et al., 2000a,b) to associate complicated spectral information with target attributes without any constraints for sample distribution (Mather, 2000). According to Kimes et al. (1998) and Lillesand and Kiefer (2000), ANNs described the intricate and complex non-linear relationships which exists between canopy-level spectral imagery and several crop conditions. Although, they have mainly been applied in classification problems, this technique has shown a great potential for continuous variable prediction problems, such as soil moisture estimation (Chang and Islam, 2000), water quality assessment (Zhang et al., 2002), biomass estimation (Jin and Liu, 1997) and yield prediction (Drummond et al., 2003; Liu et al., 2001). However, sigmoidal feed-forward neural networks or multilayer perceptrons (MLPs), which are the ANNs most used, have serious difficulties in reflecting accurately the strong interactions between input variables.

Product unit neural network (PUNN) models are an alternative to MLPs and are based on multiplicative nodes instead of additive ones. They correspond to a special class of feed-forward neural network introduced by Durbin and Rumelhart (1989). They aim to overcome the non-linear effects of variables by means of non-linear basis functions, constructed with the product of the inputs raised to arbitrary powers. These basis functions express the possible strong interactions between the variables, where the exponents may even take on real values and are suitable for automatic adjustment.

One of the main problems involved in the application of MLP and PUNN models is the selection of the most appropriate net architecture to be used. Classical neural network training algorithms assume a fixed architecture; however it is very difficult to establish beforehand the best structure of the network for a given problem. There have been many attempts to design the architecture automatically (Reed, 1993; Setiono and Hui, 1995). Evolutionary algorithms (EAs), which are stochastic search algorithms that execute a global search in the input space preventing the fall to local optimum (Angeline et al., 1994; García-Pedrajas et al., 2003; Yao, 1999), have demonstrated great accuracy in designing a near optimal architecture. This fact, together with the complexity of the error surface associated with a PUNN, justifies the use of an EA to design the structure and adjust the weights of these models (Martínez-Estudillo et al., 2006a,b).

Many researchers (Houck et al., 1996, 1997; Michalewicz, 1994) have shown that EAs perform well for global searching because they are capable of quickly finding and exploring promising regions in the search space, but they take a relatively long time to converge to a local optimum. Recently, new methods have been developed in order to improve the precision of the EAs by adding local optimization algorithms. These methods are commonly known as hybrid algorithms (Bersini and Renders, 1994). Martínez-Estudillo et al. (2006b) proposed the hybrid combination of three methods for the design of Evolutionary PUNNs (EPUNNs) for regression: an EA, a clustering process and a local search procedure. Clustering methods create groups (clusters) of mutually close points that could correspond to relevant regions of attraction. Then, local search procedures can be started once in every such region, e.g., from its centroid. They reported that the application of a clustering algorithm for selecting individuals representing the different regions in the search space was more efficient than using the optimization algorithm for every individual in the population. Their experiments in microbial growth showed that the proposed hybrid learning approach is able to obtain good results in hard real-world problems. On the other hand, this

methodology provides us with a pool of different solutions, each of them with distinct characteristics. The information contributed by all models could be combined to obtain a more effective solution of the problem.

Ensembles are another promising research field, where several models are combined to produce an answer (Dietterich, 2000). Often, the combination of individual learners outperforms the best individual among them. There are different approaches for building ANN ensembles. One of them is based on considering heterogeneous topologies, where a family of ANNs with distinct structures (and therefore complexities) are combined (Rocha et al., 2004). Since EAs design the structure of the neural nets, the models obtained at different moments in the evolution are suitable for being combined, because each of them has distinct topological characteristics.

The main objective of this work was to assess the potential of EPUNNs trained with different hybrid algorithms for reaching the best approach to the prediction of sunflower yield at field-scale using digital elevation model (DEM), *R. segetum* weed map and remote sensed information. Seven models were applied: one multivariate statistical approach (SMLR); four EPUNN models such as evolutionary programming (EP), hybrid EP (HEP), HEP with clustering (HEPC) and dynamic HEPC (DHEPC); additionally two proposals are presented for the combination of the obtained models with DHEPC, including mean DHEPC ensembles (E_{mean}) and median DHEPC ensembles (E_{median}).

2. Materials and methods

2.1. Materials and experimental design

Different types of information extracted from previous research at the study area reaching the best approach were analyzed, including aerial photography, sunflower yield data, elevation data and weed patches. The data analyzed correspond to a study conducted in 2003 at the 42 ha farm Matabueyes, located in Andalusia, Southern Spain (37.8°N, 4.8°W, WGS84), naturally infested by *R. segetum*. With a clay content of nearly 60%, the soil of Matabueyes was classified as Typic Chromoxerert (USDA-NRCS, 1998) and it is representative of the extensive dry-land of Southern Spain. Sunflower crop cultivar Jalisco was seeded at 4 kg ha^{-1} in rows 0.7 m apart in mid-March and then harvested in mid-August. Tillage production methods were applied to manage the field site. In order to control annual weed seedlings in sunflower, glyphosate (Roundup, isopropylamine salt, 360 g a.i. l^{-1}, Monsanto) was applied at pre-emergence 180 g a.i. l^{-1}, but at this rate this herbicide had no significant activity on *R. segetum* plants.

Conventional-colour (CC) and colour-infrared (CIR) aerial photographs of the studied field were taken at 15 May 2003. The photographs were taken by a turboprop twin-engine plane CESSNA 402, using an automatic pilot for managing both photographic equipment and GPS. The camera was a RMK TOP 15, with a Zeiss objective, a focal distance of 153.76 mm and Kodak Aerocolor III 2444 and Kodak Aerochrome S0734 film for CC and CIR photographs, respectively. All these photographs were taken on cloudless days between 12 and 14 h standard time and the average flight height was 1525 m to obtain photographs at a scale 1:10,000. Then, the photographs were digitalized with an AGFA Horizon A3 scanner, considering a resolution of 635 dots per inch (dpi). It is important to note that brightness and contrast were not adjusted on the digitalized images. The next step was to orthorectify the digitised images, using the fiducial marks of the aerial calibration certificate, 40 ground control points taken with a differential GPS TRIMBLE PRO-XRS equipped with a TDC-1 unit (centimetre precision) and a 10 m resolution raster DEM. Finally, images were resampled to a pixel size representing 40 cm × 40 cm ground area.

Blue (B, 400–500 nm), green (G, 500–600 nm) and red (R, 600–700 nm) bands of the electromagnetic spectrum are represented by CC photographs and green, red and near-infrared (NIR, 700–900 nm) are represented by CIR photographs. The scanner produced a RGB digital image with eight-bit true colour, so pixels of the image showed digital counts within the range of 0–255 values. These digital values are considered as being directly proportional to the total light reflected from the scene (Flowers et al., 2001).

Sunflower crop was combine-harvested in August 2003 using a Massey Fergusson® harvester equipped with a calibrated Fieldstar® yield monitor and a differential global positioning system (DGPS) receiver (Blackmore and Moore, 1999). Yield data varied from 0.50 to 2.30 tonnes ha^{-1}. The DPGS also described the elevation data (z coordinate).

R. segetum patches were mapped as described in Peña-Barragán et al. (2007), applying the Specter angle mapper (SAM) supervised classification method to the multispectral imagery, at 94% overall accuracy. SAM method considers the angle between consecutive *n*-band values as an *n*-dimensional vector, which is representative of the spectral signature of each cover-class. Smaller angles between training reference spectra and pixel to be classified represent closer coincidences. A maximum angle threshold (MAT) parameter must be specified in radians, so any pixels further away than the MAT are not classified (Kruse et al., 1993).

All spatial data from images and maps were grouping and saved to an unique multiband file, taking into account two requirements: (a) the georeference error between images was less than one pixel, so similar pixels had the same coordinate and (b) the NIR digital values of CIR photograph were corrected to digital values of CC photograph, considering the differences between the G and R bands of both original photographs. Further information about the acquisition of the photographs is described in Peña-Barragán et al. (2007).

The dataset used to train and validate the different prediction methods included all the information extracted from the different pixels of the images: red, green, blue and near-infrared digital values, elevation data, *R. segetum* infestation and yield data. Due to the very large number of pixels, the dataset was reduced by obtaining mean values for each 20 × 20 pixels of the image, resulting in a total of 1056 instances. Therefore, weed density was calculated in every grid assuming the presence of two plants per every infested pixel, which provides a conservative estimate.

The experimental design was conducted using a hold-out cross-validation procedure, where the size of training

set was approximately 3*n*/4 and *n*/4 for the generalization set, *n* being the size of the full dataset. Consequently, the above-mentioned dataset was randomly split in two datasets. A 739 instances dataset was used for model training and the remaining 317 instances formed the generalization dataset.

2.2. Methods

2.2.1. Statistical methods: stepwise multiple linear regression

SPSS 13.0 software for Windows (SPSS, 2005) was used for the SMLR model development. Regression equations were calculated for all input variables of the dataset, using a backward SMLR with the following stepwise criteria: $P \leq 0.05$ for entry and $P > 0.40$ for removal.

2.2.2. Evolutionary product unit neural networks

2.2.2.1. Product unit neural networks. PUNNs are an alternative to MLPs, and are based on multiplicative nodes instead of additives ones. A multiplicative node is given by $\prod_{i=1}^{k} x_i^{w_{ji}}$, where *k* is the number of the inputs. When the exponents w_{ji} are {0,1} a higher-order unit is obtained, namely the sigma-pi unit. The output of a polynomial or sigma-pi unit is a function of the linear sum of some monomial. In contrast to sigma-pi unit, in the product unit the exponents are not fixed and may even take real values.

Product unit based neural networks have several advantages, including increased information capacity and the ability to express strong interactions between input variables. Furthermore, it is possible to obtain upper bounds of the Vapnik–Chervonenkis (VC) dimension (Vapnik, 1999) of product unit neural networks similar to those obtained for MLP (Schmitt, 2002).

Despite these advantages, PUNNs have a major handicap: they have more local minima and a higher probability of becoming trapped in them (Ismail and Engelbrecht, 2000). The main reason for this difficulty is that small changes in the exponents can cause large changes in the total error surface and therefore their training is more difficult than the training of standard MLPs. Several efforts have been made to carry out learning methods for product units (Ismail and Engelbrecht, 1999, 2000; Janson and Frenzel, 1993). The back propagation algorithm, which is the most common algorithm for training multilayer neural networks, does not work very well with the product units because of its complex error surface.

The structure of the neural network considered is described in Fig. 1: an input layer with *k* nodes, a node for every input variable, a hidden layer with *m* nodes and an output layer with one node. There are no connections between the nodes of a layer and none between the input and output layers either. The activation function of the *j*th node in the hidden layer is given by $\prod_{i=1}^{k} x_i^{w_{ji}}$, where w_{ji} is the weight of the connection between input node *i* and hidden node *j* and $\mathbf{w}_j = (w_{j1}, \ldots, w_{jk})$ is the weight vector. The activation function of the output node is given by:

$$f(\mathbf{x}, \boldsymbol{\theta}) = \beta_0 + \sum_{j=1}^{m} \beta_j \prod_j (\mathbf{x}, \mathbf{w}_j) \quad (1)$$

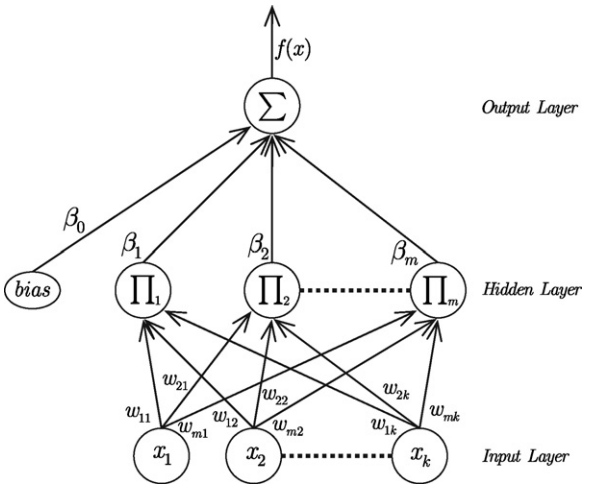

Fig. 1 – Model of a product unit based neural network.

where β_j is the weight of the connection between the hidden node *j* and the output node. The transfer function of all hidden and output nodes is the identity function.

2.2.2.2. Evolutionary algorithm. In this section we present the EA used to estimate the parameters and the structure of the PUNNs that minimizes the prediction error function. The algorithm, similar to that proposed by Martínez-Estudillo et al. (2006a), begins with the random generation of N_P individuals. Then the evolution process start and a population-update algorithm is applied. Since the algorithm falls into the class of EP paradigm (Fogel, 1995), population is subjected to the replication and mutation operations, but crossover is not considered, as this operation is usually regarded as being less effective for ANNs evolution (Angeline et al., 1994). Although there are different training methodologies for this purpose, most researchers agree that EP is the most suitable evolutionary computation paradigm for evolving neural nets (Koehn, 1994).

The general structure of the EA is detailed next:

Evolutionary programming (EP):

(1) Generate a random population of size N_P.
(2) Repeat until the stopping criterion is fulfilled.
  (2a) Apply parametric mutation to the best 10% of individuals. Apply structural mutation to the remaining 90% of individuals.
  (2b) Calculate the fitness of every individual in the population.
  (2c) Add best *fitness* individual of the last generation (*elitist algorithm*).
  (2d) Rank the individuals with respect to their *fitness*.
  (2e) Best 10% of population individuals are replicated and substitute the worst 10% of individuals.
(3) Select the best individual of the population in the last generation and return it as the final solution.

First, the initial population is generated: the algorithm begins with the random generation of a larger number of networks than the number used during the evolutionary pro-

cess. Ten N_P networks are generated, where N_P is the number of individuals of the population to be trained during the evolutionary process. Fitness of a neural network of the population that implements a function $f(x)$, is calculated using a $D = \{(\mathbf{x}_l, y_l); l = 1, 2, \ldots, n_T\}$ training dataset, where the number of samples is n_T. Mean squared error (MSE) of $f(x)$ is considered:

$$\mathrm{MSE}(f) = \frac{1}{n_T}\sum_{l=1}^{n_T}(y_l - f(x_l))^2 \quad (2)$$

where y_l are the observed values and $f(x_l)$ are the predicted values. The fitness function $A(f)$ is defined by means of a strictly decreasing transformation of the MSE:

$$A(f) = \frac{1}{1 + \mathrm{MSE}(f)}, \quad 0 < A(f) \leq 1 \quad (3)$$

The adjustment of both weights and structure of the PUNNs is performed by the complementary action of two mutation operators: parametric and structural mutation. Parametric mutation implies a modification in the coefficients (β_j) and the exponents (w_{ji}) of the model, using a self-adaptive simulated annealing algorithm (Kirkpatrick et al., 1983). Structural mutation modifies the topology of the neural nets, helping the algorithm to avoid local minima and increasing the diversity of the trained individuals. Five structural mutations are applied sequentially to each network: node deletion, connection deletion, node addition, connection addition and node fusion. When node deletion is applied, number of hidden nodes to be removed is obtained as a uniform value in a previous specified interval. Apart from this mutation, if connection deletion is applied, the number of connections to be deleted in the neural net is also obtained as a uniform value, but in this case, as the mutation is less disruptive, the selected interval uses to be a wider one. More details about the EA can be found in Martínez-Estudillo et al. (2006a).

2.2.2.3. Hybrid evolutionary programming algorithms. In this work, different variants of hybrid EAs have been applied, all of them proposed by Martínez-Estudillo et al. (2006b). The EP algorithm is the EA exposed in the previous section without neither a local search nor a clustering process. In the hybrid EP (HEP), the EP is run without the local optimization algorithm and then it is applied to the best solution obtained by the EP in the final generation. This allows the precise local optimum around the final solution to be found. Another version of hybrid EA is the HEP with the clustering algorithm (HEPC), which applies the clustering process over a large enough subset of the best individuals in the final population. The number of individuals in this subset and number of clusters to be created are critical parameters of the clustering process. Once clusters have been determined, the best individual in each cluster is selected and then optimized using the local search algorithm. Finally, dynamic HEP with clustering (DHEPC) is the most sophisticated algorithm. It carries out both the clustering process and local search dynamically during the evolution every G_0, where G_0 must be fixed a priori. All optimized individuals are extracted and stored and the final solution is the best local optimum among them.

The main objective of these methodologies is to reduce the number of times it is necessary to apply the local optimization procedure, since local search algorithms commonly involve a high computational cost. The clustering process selects the most representative groups of the population, providing a subset of individuals with different features. The selected clustering method selected is k-means clustering, using a distance measure defined for the vectors of the different values obtained for each individual over the training dataset. Further information can be found in Martínez-Estudillo et al. (2006b).

The local optimization procedure considered is the *Levenberg–Marquardt* (L–M) *algorithm* (Marquardt, 1963), a gradient-based methodology, designed specifically for minimizing a MSE (Bishop, 1995). The LM method can be trapped in a local optimum. Moreover, PUNNs have a very complex error surface with many minimum optima and local plateau. That is the reason why it is necessary to apply the *L–M algorithm* at different points of the evolution, so global optimum can be discovered with a higher probability.

The hybrid algorithms applied are summarized as follows:

Hybrid evolutionary programming (HEP):

(1) Generate a random population of size N_P.
(2) Repeat EP algorithm until the stopping criterion is fulfilled.
(3) Apply *L–M algorithm* to best solution obtained in the EP algorithm.
(4) Return the optimized individual as the final solution.

Hybrid evolutionary programming with clustering (HEPC):

(1) Generate a random population of size N_P.
(2) Repeat EP algorithm until the stopping criterion is fulfilled.
(3) Apply k-means process to best N_C individuals of the population in the last generation and assign a cluster to each individual.
(4) Apply *L–M algorithm* to best solution obtained in each cluster.
(5) Select the best individual among optimized ones and return it as the final solution.

Dynamic hybrid evolutionary programming with clustering (DHEPC):

(1) Generate a random population of size N_P.
(2) Repeat EP algorithm until the stopping criterion is fulfilled, applying the following process every G_0 generations:
  (2a) Apply k-means process to best N_C individuals of the population in current generation, assigning a cluster to each individual.
  (2b) Apply *L–M algorithm* to best solution obtained in each cluster.
  (2c) Select the best individual among optimized ones and add it to B set.
(3) Select best individual in B set and return it as the final solution.

2.2.2.4. Ensemble approaches. All above-mentioned methodologies share the risk of over fitting training dataset. A local search procedure leads us to the closer local optimum from the current location in the training set, but sometimes the

optimized model loses its generalization capability. In this paper, ensembles are presented as a way of avoiding this overfitting, by the combination of all different EPUNN models obtained through the evolution process. Considering the models obtained in different generations, a pool of individuals with different structures can be constructed and applied to the data as an ensemble. Models are extracted from the DHEPC algorithm at different moments in the evolution, so the set of individuals obtained will presumably gather neural nets with the most efficient and varied topologies for solving the problem.

For combining outputs of all regression models of the ensemble, two different proposals are considered: mean DHEPC ensembles (E_{mean}) and median DHEPC ensembles (E_{median}). Let $B = \{f_k\}$, for $k = 1, \ldots, s$, be the set of optimized solutions obtained throughout the evolution process in a run of the DHEPC algorithm. The output of E_{mean} ensemble is calculated as the mean value of all the outputs of the elements of B and E_{median} output is obtained as the median of the outputs of the elements of B:

$$E_{mean}(B, x_l) = \overline{f(x_l)}, \qquad E_{median}(B, x_l) = f_M(x_l) \tag{4}$$

where $\overline{f(x_l)}$ and $f_M(x_l)$ represents the mean an median values of $f_k(x_l)$ values, which are obtained using Eq. (1).

2.2.3. Model development and evaluation

To start processing data, each of the input variables was scaled in the ranks [0.1,1.1]. The lower bound is chosen to avoid inputs values near to 0 that can produce very large values of the function for negative exponents. The upper bound is chosen near 1 to avoid dramatic changes in the outputs of the network when there are weights with large values (especially in the exponents). The new scaled variables were named Weed*, Z^*, R^*, G^*, B^* and NIR*. For example, Z^* is calculated as follows:

$$Z^* = \frac{Z - Z_{min}}{Z_{max} - Z_{min}} + 0.1 \tag{5}$$

where Z is the original elevation. Z_{min} and Z_{max} are the minimum and maximum values in the whole dataset.

As was mentioned before, SPSS 13.0 software for Windows (SPSS, 2005) was used for the SMLR model development. The different EPUNN experiments were conducted using a software package developed in JAVA by the authors, as an extension of JCLEC framework (http://jclec.sourceforge.net/) (Ventura et al., 2007). The software package is available in the non-commercial JAVA tool named KEEL (http://www.keel.es). The parameters used in the evolutionary algorithm for learning the EPUNN models are common for all methodologies: the $\mathbf{w}_j$ vector and the coefficients β_j are initialized in the [−5,5] interval; the maximum number of hidden nodes is $m = 6$; the size of the population is $N_P = 1000$. The number of nodes that can be added or removed in a structural mutation is within the [1,3] interval, whereas the number of connections that can be added or removed in a structural mutation is within the [1,7] interval. The only parameter of the L–M algorithm is the tolerance of the error to stop the algorithm; in our experiment, this parameter has the value 0.01. The k-means algorithm is applied to $N_C = 250$ best individuals in the population. The number of clusters is 4 for both the HEPC and DHEPC algorithms. For this latter algorithm, $G_0 = 600$. Finally, it is important to note that, as an evolutionary method has been applied for optimizing weights of the neural nets, a learning rate parameter is not considered and weight optimization is achieved through the double effect of parametric mutations and *Levenberg–Marquardt* local search algorithm.

Models obtained with the different evolutionary and statistical methodologies are evaluated using their prediction error over the training and generalization sets. Two error measurements are considered: the root mean squared error (RMSE, $RMSE(f) = \sqrt{MSE(f)}$, see Eq. (2)) and the standard error of prediction (SEP). Let $D = \{(x_i, y_i);\ l = 1, \ldots, n_T\}$ be the dataset. The SEP of a model that implements a function $f(x)$ represents a percentage error over the dataset and can be expressed as:

$$SEP(f) = \frac{100}{|\bar{y}|}\sqrt{MSE(f)} \tag{6}$$

where $\bar{y}$ is the average output of all patterns in dataset.

3. Results and discussion

Results obtained with the different modelling approaches were evaluated by using both RMSE and SEP, and a regression between observed and simulated yields was performed to verify that compared models did a comparable job. Table 1 shows the statistical results of the four EPUNN algorithms (EP, HEP, HEPC and DHEPC) and the combination of the obtained models with DHEPC (E_{mean} and E_{median}) over 30 runs. Based on these results, it is can be concluded that DHEPC, E_{mean} and E_{median} clearly outperform the remainder methodologies, so we used the analysis of variance (ANOVA) technique to ascertain the statistical significance of observed differences between the three corresponding means, assuming that the $RMSE_G$ values obtained have a normal distribution; a Kolmogorov–Smirnov test for normality was reached for DHEPC, E_{mean} and E_{median} with P-values of 0.650, 0.965 and 0.999, respectively. The ANOVA involves a linear regression model in which, $RMSE_G$ is the dependent variable and the independent variable is the type of algorithm. The comparisons were made in terms of a critical level for Snedecor's F. If the significance level, α, was higher than this critical level, P, we rejected the hypothesis of identical $RMSE_G$'s means. In our case this hypothesis is accepted because the P-value is 0.178, higher than a standard $\alpha = 0.05$. Finally, we used an independent t-test for analyzing the significant difference between the means of DHEPC and E_{mean} algorithms. It can be seen, for $\alpha = 0.1$, that differences in variance existed from a prior Levene's test (P-value = 0.061), and that there were differences in mean (P-value = 0.08). Based on these results, the E_{mean} methodology should be adopted for predicting sunflower yield production, since it is significantly more accurate (lower values) than DHEPC, both in terms of mean and standard deviation. Comparing E_{mean} and E_{median} algorithms, there are no significant differences neither in terms of mean nor standard deviation, but the best result ($RMSE_G = 0.2119$ tonnes ha^{-1}) is obtained by E_{mean} methodology.

A performance comparison between proposed EPUNN models and a SMLR model measured by using the mean RMSE

Table 1 – Statistical results over 30 runs of the different evolutionary methodologies

Algorithms	RMSE (tonnes ha^{-1})							
	Learning				Generalization			
	Mean	S.D.	Best	Worst	Mean	S.D.	Best	Worst
EP	0.2356	0.0469	0.2274	0.2427	0.228	0.0566	0.2177	0.2406
HEP	0.2254	0.0374	0.2214	0.2349	0.22	0.04	0.2138	0.23
HEPC	0.2249	0.0374	**0.2209**[a]	0.2349	0.22	0.04	0.2131	0.2298
DHEPC	**0.2238**	**0.03**	**0.2209**	**0.2280**	0.2191	0.0346	0.2152	0.2241
E_{mean}	0.2243	0.0316	0.2211	0.2302	**0.2179**	**0.03**	**0.2119**	**0.2214**
E_{median}	0.2245	0.0332	0.2211	0.2315	0.2184	**0.03**	0.2131	0.222

RMSE, Root mean squared error; S.D., standard deviation; EP, evolutionary programming; HEP, hybrid evolutionary programming; HEPC, hybrid evolutionary programming with clustering; DHEPC, dynamic hybrid evolutionary programming; E_{mean}, mean DHEPC ensembles; E_{median}, median DHEPC ensembles.

[a] The values given in bold represent 'best RMSE'.

value and SEP in the generalization and learning dataset is shown in Table 2. The best single EPUNN obtained in all runs of the different algorithms is considered, corresponding to DHEPC methodology. In both cases, the models developed produced relatively low values for RMSE (<0.2594 tonnes ha^{-1}), which means that relatively low sunflower yield prediction error was achieved. However, the lowest mean RMSE and SEP for the learning and generalization dataset were obtained with the EPUNN model, SEP being around 16%. The highest RMSE was achieved for SMLR (SEP about 19% for learning and generalization). These results support the findings of other authors, which obtained similar SEP values as reported by Uno et al. (2005). They compared SMLR and ANN approaches along with various vegetation indices to develop corn yield prediction methods. They did not find clear differences between ANNs and SMLR (about 20% validation MSE in both models), although greater prediction accuracy was obtained with ANNs than with empirically derived vegetation indices. Since RMSE values depend on the magnitude of the data, SEP values provided better comparisons between different models. In our case, difference between EPUNN and SMLR models in sunflower yield prediction was about 0.0403 tonnes ha^{-1} (3.02%) in generalization RMSE (Table 2).

Regression parameters for observed and simulated sunflower yields for the worst and best models are shown in Fig. 2. The EPUNN model, with an approximately two times higher R^2 value, showed a higher goodness of fit with a closer cluster along the best-fit line than SMLR. However, both models presented high deviations between observed and predicted values, these differences being more noticeable for lowest yield values. The EPUNN best-fit regression equation slope was closer to 1 than the SMLR slope and the intercept closer to 0 than that of SMLR. The SMLR model performed the worst probably due to the higher values of sunflower yield being overestimated, i.e. they were higher than the best-fit line as can be seen in Fig. 2a. Nevertheless, higher predicted yields were at a similar distance from the regression line of EPUNN model (Fig. 2b).

Regression equations of the best and worst models for yield prediction are presented in Table 3. SMLR model identified the elevation (*Z*) to be the top important factor, meaning that sunflower yield was lower at higher elevation. This can be observed in Fig. 3, where a yield map with the predictions of the EPUNN model and an *R. segetum* weed map are presented. The yield reduction at higher elevation was probably due to the limited water supply in these regions, as has previously been reported for corn and soybean yield (Kravchenko and Bullock, 2002a,b; Miao et al., 2006). Weed infestation was selected as being the second most important factor to predict sunflower yield. Classic *R. segetum*–sunflower competition models for predicting sunflower yield without considering any spatial or spectral components assumed a non-linear hyperbolic relationship between mean *R. segetum* densities, obtaining a much higher RMSE (about 1.1 tonnes ha^{-1}) (Carranza et al., 1995) than RMSE of methods herein compared. Fig. 3 clearly shows that lower sunflower yield is located where *R. segetum* patches appear. For the SMLR model, regression equations shown in Table 3 indicate that one of the factors affecting sunflower

Table 2 – Comparative performance of the best EPUNN model and the SMLR model

Models	Model performance			
	Learning		Generalization	
	RMSE (tonnes ha^{-1})	SEP (%)	RMSE (tonnes ha^{-1})	SEP (%)
SMLR	0.2594	19.37	0.2534	19.07
EPUNN	**0.2256**[a]	**16.85**	**0.2131**	**16.05**

Regression equations of the best EPUNN model and the SMLR model. RMSE, Root mean squared error; SEP, standard error of prediction; SMLR, stepwise multiple linear regression; EPUNN, evolutionary product unit neural network.

[a] The values given in bold represent 'best performance'.

Table 3 – Regression equations of the best EPUNN model and the SMLR model

Models	Regression equation
SMLR	Yield (tonnes ha^{-1}) = 3.7031 − 0.0097Weed − 0.0133Z − 0.0033R + 0.0003NIR
EPUNN	Yield (tonnes ha^{-1}) = 1.6973 + 0.7396h_1 − 0.0709h_2 − 13.1973h_3 + 33.8768h_4 − 22.3513h_5 $h_1 = (G^*)^{6.1364}(Z^*)^{-1.1831}(\text{Weed}^*)^{0.4289}$ $h_2 = (\text{NIR}^*)^{-0.7263}(R^*)^{6.2797}(B^*)^{-2.3923}(Z^*)^{-2.1374}(\text{Weed}^*)^{0.5795}$ $h_3 = (\text{NIR}^*)^{-0.0902}(R^*)^{2.8042}(G^*)^{-0.3956}(B^*)^{1.6049}(Z^*)^{0.9406}$ $h_4 = (R^*)^{1.5069}(B^*)^{2.9757}(Z^*)^{0.5926}(\text{Weed}^*)^{0.0552}$ $h_5 = (\text{NIR}^*)^{0.0758}(G^*)^{0.9941}(B^*)^{3.7274}(Z^*)^{0.3144}(\text{Weed}^*)^{0.1106}$

SMLR, Stepwise multiple linear regression; EPUNN, evolutionary product unit neural network; Weed, *R. segetum* density (number of plants m^{-2}); Z, elevation (m); R, G, B, NIR, scaled digital values of red (R), green (G), blue (B) and near infrared (NIR) bands. Scaled variables Weed*, Z*, R*, G*, B* and NIR* ∈ [0.1,1.1].

yield is weed infestation but it is not the only one or the most influential. It is widely accepted that vigorous and healthy crops usually show high reflectance in near infrared and low in red (Hatfield and Pinter, 1993); that is represented in the SMLR equation, where R and NIR variables also affect to the prediction, although they have a more reduced influence.

The EPUNN model produced a regression equation with higher level of complexity and provided much more information about the relationship between spectral factors and crop yield than the SMLR model. In general, a neural network produces equations that are difficult to understand. The structure of the interconnected neurons depends on the complexity of a given problem and the number of neurons in the hidden layers is related to the performance of a neural network. Too few hidden neurons limit the ability of the network to model the problem, and too many result in overtraining of the input/output pair patterns presented in the training process. In our case, EPUNN formulas are not particularly complex, since they have neither a very high number of neurons nor too many variables associated in each neuron. As can be observed in Table 3, the EPUNN model has six elements, the first one (1.6973 tonnes ha^{-1}) corresponding to the bias value and the other corresponding to the hidden neurons (h_i, $1 \le i \le 5$). The influence of the input parameters on the output depends not only on the value of their exponents but also on the coefficient corresponding to the hidden neurons in which they

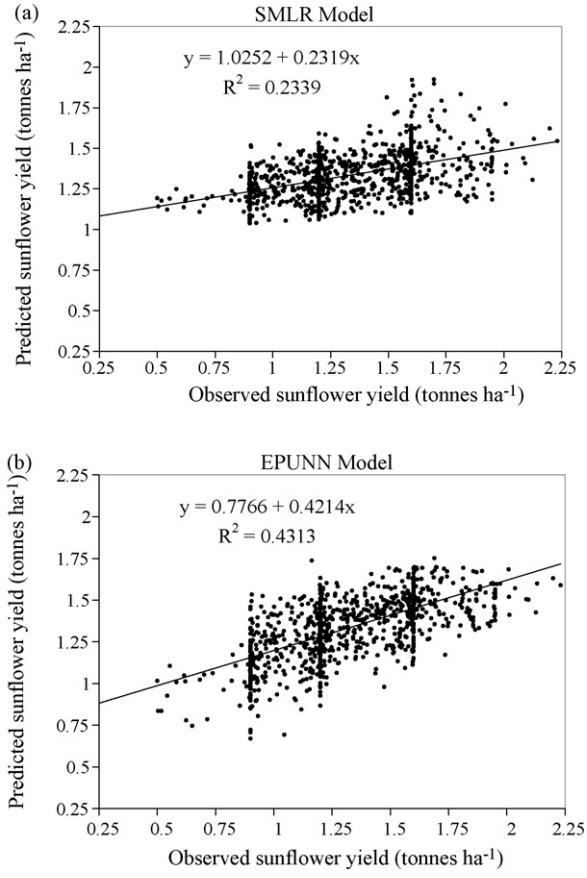

Fig. 2 – Scatter-plot of observed and computed sunflower yield using the developed models on complete set of data: (a) SMLR model and (b) EPUNN model.

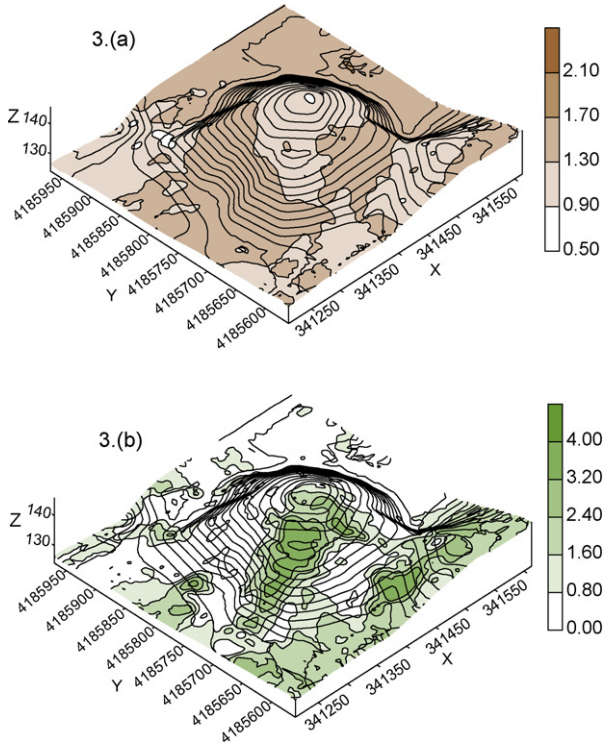

Fig. 3 – (a) Sunflower yield map predicted with EPUNN model (tonnes ha^{-1}) and (b) *R. segetum* weed map (plants m^{-2}).

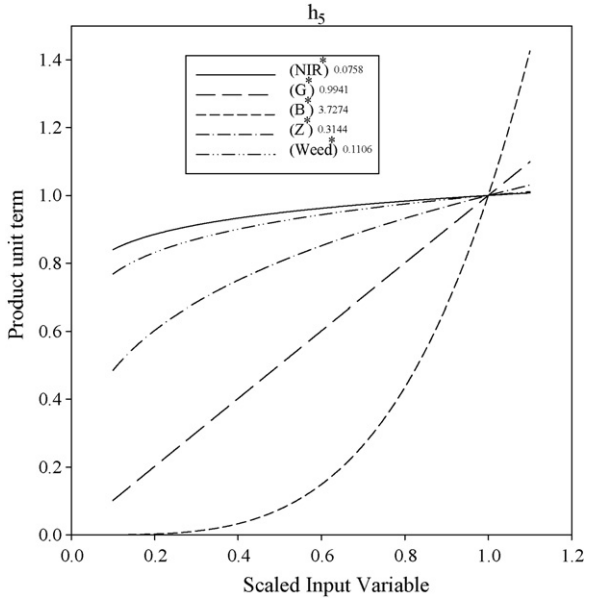

Fig. 4 – Relative contribution of h_5 hidden neuron terms used by the EPUNN model, h_5 bearing an inverse linear relationship with sunflower crop yield.

are represented. Consequently, in order to derive agronomical information by using the EPUNN model, the response of each PU hidden neuron must be independently studied. As an example, h_5 product unit terms affected by its exponent were plotted versus the scaled input variables (Weed*, Z^*, G^*, B^* and NIR*) over the range [0.1,1.1] (see Fig. 4). From the EPUNN equation shown in Table 3, it follows that the sunflower crop yield depends mainly on the interaction between the variables R^*, G^*, B^* and Z^*, the contribution of Weed* and NIR* being practically negligible, as inferred from the low exponential values of these variables in all hidden neurons. As can be observed in Fig. 4, h_5 value, which bear an inverse relationship with sunflower crop yield, is larger when Z^*, B^* and G^* increases and exponents of NIR* and Weed* variables make their contribution in the hidden neuron output non-significant, as their weighted values are near to 1. From the equation shown in Table 3, it follows that R^* variable only appears in the hidden neurons with negative coefficient, and its exponents are always greater than 0. Therefore, crop yield is inversely related to R^* value. In summary, although NIR* and weed infestation (Weed*) were also selected in EPUNN model, the wavebands of visible spectral window (B^*, G^* and R^*) and elevation (Z^*) were identified as the most influent parameters. The parameters R^*, G^*, B^* and Z^* are the key for the determination of sunflower crop yield when using EPUNN model, being yield larger when Z^*, B^*, R^* and G^* decreases. Results from other authors agree with these relationships between sunflower crop and visible domain (Peña-Barragán et al., 2006) and Z values (Ruiz et al., 2007).

Over the years, the creation of accurate maps using harvested-mounted crop yield-monitoring systems has been essential for successful implementation of precision farming (Blackmore and Moore, 1999; Reitz and Kutzbach, 1996). Our results demonstrate that models integrating spectral data, *R. segetum* spatial infestation and elevation, fit good models for predicting sunflower yield over a large area. It can be concluded that the SMLR model is capable of achieving a higher overall performance than previous classic studies, but does not achieve such high prediction accuracy as EPUNN. It is important to consider that DHEPC models are obtained from EP models, the additional computational requirements being nearly insignificant regarding the achieved improvement in accuracy performance. Once EPUNNs has been shown to successfully predict sunflower yield maps by using primarily spectral data from airborne multispectral imagery, the next investigation could address the examination of QuickBird satellite imagery for mapping sunflower yield in larger areas (of at least over 64 km^2), since QuickBird provides four channels (*B*, *G*, *R* and NIR) of multispectral imagery with 2.4 m of spatial resolution and has shown to be a useful data source for determining sorghum yield (Yang et al., 2006).

4. Conclusions

This study demonstrated the capability of EPUNN to analyze multispectral imagery, weed and elevation data for predicting sunflower yield in early growth stage. EPUNN provided better accuracy than linear SMLR models both in training set (16.85%) and generalization set (16.05%). Moreover, four different EPUNN algorithms (EP, HEP, HEPC and DHEPC) were evaluated in training PUNN for the sunflower yield prediction problem and two methods for combining resulting DHEPC models were proposed and compared to the remaining EPUNN algorithms. The statistical results of the multiple comparison tests carried out show that E_{mean} and E_{median} yielded better results than the other algorithms, with lower RMSE mean and standard deviation.

From an agronomic point of view, our study demonstrated that sunflower prediction yield in infested *R. segetum* fields is affected by weed infestation, but also implies complex relationship among parameters such as elevation or digital (or spectral) data. Granted that, computational requirements for EP were much higher than for SMLR, those necessary for DHEPC were nearly insignificant. Thus, taking into account that precision agriculture management requires a great accuracy, the criteria for selection SMLR or EPUNNs models should not be based on decreasing computational requirements and complexity, but on the accuracy of prediction. Although the results of this study are promising in considering the multivariate agronomic context, more research is needed to work on a larger field surface using high spatial resolution satellite imagery.

Acknowledgements

This work has partially been financed by TIN2005-08386-C05-02 and AGL-2005-06180-CO3-02, projects of the Spanish Inter-Ministerial Commission of Science and Technology and FEDER funds. The research of Dr. M. Jurado-Expósito and P.A. Gutiérrez has been supported by "Ramón y Cajal" (MEC) and I3P-Predoctoral Programs, respectively.

REFERENCES

Angeline, P.J., Saunders, G.M., Pollack, J.B., 1994. An evolutionary algorithm that constructs recurrent neural networks. IEEE Trans. Neural Networks 5 (1), 54–65.

Bersini, H., Renders, B., 1994. Hybridizing genetic algorithms with hill-climbing methods for global optimization: two possible ways. In: Proceedings of the IEEE International Symposium on Evolutionary Computation, Orlando, Florida, pp. 312–317.

Bishop, M., 1995. Neural Networks for Pattern Recognition. Oxford University Press, UK.

Blackmore, S., Moore, M., 1999. Remedial correction of yield map data. Precis. Agric. 1 (1), 53–66.

Burks, T.F., Shearer, S.A., Green, J.D., Heath, J.R., 2002. Influence of weed maturity levels on species classification using machine vision. Weed Sci. 50 (6), 802–811.

Carranza, P., Saavedra, M., García-Torres, L., 1995. Competition between *Ridolfia segetum* and sunflower. Weed Res. 35 (5), 369–376.

Castro-Tendero, A.J., García-Torres, L., 1995. SEMAGI—an expert system for weed control decision. Crop Protect. 14 (7), 543–548.

Chang, D.H., Islam, S., 2000. Estimation of soil physical properties using remote sensing and artificial neural network. Remote Sens. Env. 74 (3), 534–544.

Cho, S.I., Lee, D.S., Jeong, J.Y., 2002. Weed-plant discrimination by machine vision and artificial neural networks. Biosyst. Eng. 83 (3), 275–280.

Dietterich, T.G., 2000. Ensemble Methods in Machine Learning. In: Kittler, J., Roli, F. (Eds.), Proceedings of the First International Workshop on Multiple Classifier Systems, Lecture Notes in Computer Science, 1857. Springer Verlag, New York, pp. 1–15.

Drummond, S.T., Sudduth, K.A., Joshi, A., Birrell, S.J., Kitchen, N.R., 2003. Statistical and neural methods for site-specific yield prediction. Trans. ASAE 46 (1), 5–14.

Durbin, R., Rumelhart, D., 1989. Products units: a computationally powerful and biologically plausible extension to backpropagation networks. Neural Comput. 1 (1), 133–142.

Flowers, M., Weisz, R., Heiniger, R., 2001. Remote sensing of winter wheat tiller density for early nitrogen application decisions. Agron. J. 93 (4), 783–789.

Fogel, D.B., 1995. Evolutionary Computation: Toward a New Philosophy of Machine Intelligence. IEEE Press, New York.

Friedman, J., Stuetzle, W., 1981. Projection pursuit regression. J. Am. Stat. Assoc. 76, 817–823.

García-Pedrajas, N., Hervás-Martínez, C., Muñoz-Pérez, J., 2003. Covnet: a cooperative coevolutionary model for evolving artificial neural networks. IEEE Trans. Neural Networks 14 (3), 575–596.

Goel, P.K., Prasher, S.O., Patel, R.M., Landry, J.A., Bonnell, R.B., Viau, A.A., 2003. Classification of hyperspectral data by decision trees and artificial neural networks to identify weed stress and nitrogen status of corn. Comput. Electron. Agric. 39 (2), 67–93.

Hastie, T.J., Tibshirani, R.J., 1990. Generalized Additive Models. Chapman & Hall, London.

Hatfield, J.L., Pinter, P.J., 1993. Remote sensing for crop protection. Crop Protect. 12 (6), 403–413.

Houck, C.R., Joines, J.A., Kay, M.G., 1996. Comparison of genetic algorithms, random start, and two-opt switching for solving large location–allocation problems. Comput. Oper. Res. 23 (6), 587–596.

Houck, C.R., Joines, J.A., Kay, M.G., Wilson, J.R., 1997. Empirical investigation of the benefits of partial Lamarckianism. Evol. Comput. 5 (1), 31–60.

Ismail, A., Engelbrecht, A.P., 1999. Training product units in feedforward neural networks using particle swarm optimisation. In: Proceedings of the International Conference on Artificial Intelligence, Durban, South Africa.

Ismail, A., Engelbrecht, A.P., 2000. Global optimization algorithms for training product unit neural networks. In: Proceedings of the International Joint Conference on Neural Networks (IJCNN'2000), vol. 1, Como, Italy, pp. 132–137.

Janson, D.J., Frenzel, J.F., 1993. Training product unit neural networks with genetic algorithms. IEEE Exp. 8 (5), 26–33.

Jin, Y.Q., Liu, C., 1997. Biomass retrieval from high-dimensional active/passive remote sensing data by using artificial neural networks. Int. J. Remote Sens. 18 (4), 971–979.

Jurado-Expósito, M., López-Granados, F., Peña-Barragán, J.M., García-Torres, L., 2005. Weed density prediction with secondary input of DEM information. In: Stafford, J. (Ed.), Proceedings of the Fifth European Conference on Precision Agriculture. Uppsala, Sweden, pp. 115–122.

Karimi, Y., Prasher, S.O., McNairn, H., Bonnell, R.B., Dutilleul, P., Goel, P.K., 2005. Classification accuracy of discriminant analysis, artificial neural networks, and decision trees for weed and nitrogen stress detection in corn. Trans. ASAE 48 (3), 1261–1268.

Kenkel, N.C., Derksen, D.A., Thomas, A.G., Walson, P.R., 2002. Review: multivariate analysis in weed science research. Weed Sci. 50 (3), 281–292.

Kimes, D.S., Nelson, R.F., Manry, M.T., Fung, A.K., 1998. Attributes of neural networks for extracting continuous vegetation variables from optical and radar measurements. Int. J. Remote Sens. 19 (14), 2639–2663.

Kirkpatrick, S., Gelatt, C.P., Vecchi, M.P., 1983. Optimization by simulated annealing. Science 220 (4598), 671–680.

Koehn, P., 1994. Combining genetic algorithms and neural networks: the encoding problem. Ph.D. Thesis. University of Erlangen and University of Tennessee, Knoxville.

Kravchenko, A.N., Bullock, D.G., 2002a. Spatial variability of soybean quality data as a function of field topography. I. Spatial data analysis. Crop Sci. 42 (3), 804–815.

Kravchenko, A.N., Bullock, D.G., 2002b. Spatial variability of soybean quality data as a function of field topography. II. A proposed technique for calculating the size of the area for differential soybean harvest. Crop Sci. 42 (3), 816–821.

Kruse, F.A., Lefkoff, A.B., Boardman, J.B., Heidebrecht, K.B., Shapiro, A.T., Barloon, P.J., Goetz, A.F.H., 1993. The spectral image processing system (SIPS)—interactive visualization and analysis of imaging spectrometer data. Remote Sens. Env. 44 (2), 145–163.

Lillesand, T.M., Kiefer, R.W., 2000. Remote Sensing and Image Interpretation. Wiley, New York.

Liu, J., Goering, C.E., Tian, L., 2001. A neural network for setting target corn yields. Trans. ASAE 44 (3), 705–713.

Liu, Z., Clay, S.A., Clay, D.A., 2002. Spatial variability of atrazine and alachlor efficacy and mineralization in an eastern South Dakota field. Weed Sci. 50 (5), 662–671.

Marquardt, D.W., 1963. An algorithm for least-squares estimation of non-linear parameters. J. Soc. Ind. Appl. Math. 11 (2), 431–441.

Martínez-Estudillo, A.C., Mártínez-Estudillo, F.J., Hervás-Martínez, C., García-Pedrajas, N., 2006a. Evolutionary product unit based neural networks for regression. Neural Networks 19 (4.), 477–486.

Martínez-Estudillo, A.C., Hervás-Martínez, C., Martínez-Estudillo, F.J., García-Pedrajas, N., 2006b. Hybridization of evolutionary algorithms and local search by means of a clustering method. IEEE Trans. Syst. Man Cybernet. 36 (3), 534–545.

Mather, P.M., 2000. Computer Processing of Remotely Sensed Images: An Introduction. Wiley, Chichester, UK.

Miao, Y., Mulla, D.J., Robert, P.C., 2006. Identifying important factors influencing corn yield and grain quality variability using artificial neural networks. Precis. Agric. 7 (2), 117–135.

Michalewicz, Z., 1994. Genetic Algorithms + Data Structures = Evolution Programs. Springer Verlag, New York.

Osborne, S.L., Schepers, J.S., Francis, D.D., Schlemmer, M.R., 2002. Use of spectral radiance to estimate in-season biomass and grain yield in nitrogen- and water-stressed corn. Crop Sci. 42 (1), 165–171.

Peña-Barragán, J.M., López-Granados, F., Jurado-Expósito, M., García-Torres, L., 2006. Spectral discrimination of *Ridolfia segetum* and sunflower as affected by phenological stage. Weed Res. 46 (1), 10–21.

Peña-Barragán, J.M., López-Granados, F., Jurado-Expósito, M., García-Torres, L., 2007. Mapping *Ridolfia segetum* Moris patches in sunflower (*Helianthus annuus* L.) crop using aerial photographs. Weed Res. 47 (2), 164–172.

Pilesjö, P., Thylén, L., Persson, A., 2005. Topographical data for delineation of agricultural management zones. In: Stafford, J. (Ed.), Proceedings of the Fifth European Conference on Precision Agriculture. Uppsala, Sweden, pp. 819–826.

Plant, R.E., 2001. Site-specific management: the application of information technology to crop production. Comput. Electron. Agric. 30 (1), 9–29.

Reed, R., 1993. Pruning algorithms: a survey. IEEE Trans. Neural Networks 4 (5), 740–747.

Reitz, P., Kutzbach, H.D., 1996. Investigations on a particular yield mapping system for combine harvesters. Comp. Electron. Agric. 14 (2/3), 137–150.

Rocha, M., Cortez, P., Neves, J., 2004. Ensembles of artificial neural networks with heterogeneous topologies. In: Proceedings of the Fourth Symposium on Engineering of Intelligent Systems, Madeira.

Ruiz, D., Escribano, C., Fernández-Quintanilla, C., 2007. Identifying associations among sterile oat (*Avena sterilis*) infestation level, landscape characteristics, and crop yields. Weed Sci. 54 (6), 1113–1121.

Schmitt, M., 2002. On the complexity of computing and learning with multiplicative neural networks. Neural Comput. 14 (2), 241–301.

Setiono, R., Hui, L.C.K., 1995. Use of quasinewton method in a feedforward neural-network construction algorithm. IEEE Trans. Neural Networks 6 (1), 273–277.

Shanin, M.A., Tollner, E.W., McClendon, R.W., Arabnia, H.R., 2002. Apple classification based on surface bruises using image processing and neural networks. Trans. ASAE 45 (5), 1619–1627.

Shibayama, M., Akiyama, T., 1991. Estimating grain yield of maturing rice canopies using high spectral resolution reflectance measurements. Remote Sens. Env. 36 (1), 45–53.

SPSS, 2005. Advanced Models. Copyright 13.0 SPSS Inc., Chicago, IL.

Uno, Y., Prasher, S.O., Lacroix, R., Goel, P.K., Karimi, Y., Viau, A., Patel, R.M., 2005. Artificial neural networks to predict corn yield from compact airborne spectrographic imager data. Comput. Electron. Agric. 47 (2), 149–161.

USDA-NRCS, 1998. Keys to Soil Taxonomy, eighth ed. USDA-NRCS, Washington, DC, USA.

Vapnik, V.N., 1999. The Nature of Statistical Learning Theory. Springer, New York.

Ventura, S., Romero, C., Zafra, A., Delgado, J.A., Hervás-Martínez, C. JCLEC: a JAVA framework for evolutionary computation. Soft Computing (2007), published on line.

Yang, C., Prasher, S.O., Landry, J.A., Ramaswamy, H.S., Ditommaso, A., 2000a. Application of artificial neural networks in image recognition and classification of crop and weeds. Can. Agric. Eng. 42 (3), 147–152.

Yang, C., Everitt, J.H., Bradford, J.M., Escobar, D.E., 2000b. Mapping grain sorghum growth and yield variations using airborne multispectral digital imagery. Trans. ASAE 43 (6), 1927–1938.

Yang, C., Bradford, J.M., Wiegand, C.L., 2001. Airborne multispectral imagery for mapping variable growing conditions and yields of cotton, grain sorghum, and corn. Trans. ASAE 44 (6), 1983–1994.

Yang, C., Everitt, J.H., Bradford, J.M., 2006. Comparison of QuickBird satellite imagery and airborne imagery for mapping grain sorghum yield patterns. Precis. Agric. 7 (1), 33–44.

Yao, X., 1999. Evolving artificial neural networks. Proc. IEEE 87 (9), 1423–1447.

Zhang, Y., Pulliainen, J., Koponen, S., Hallikainen, M., 2002. Application of an empirical neural network to surface water quality estimation in the Gulf of Finland using combined optical data and microwave data. Remote Sens. Env. 81 (2/3), 327–336.